Journal of Power Sources 182 (2008) 565–579

Contents lists available at ScienceDirect

Journal of Power Sources

journal homepage: www.elsevier.com/locate/jpowsour

Passively operated vapor-fed direct methanol fuel cells for portable applications

Steffen Eccarius [a,*], Falko Krause [a], Kevin Beard [b], Carsten Agert [a]

[a] Fraunhofer Institute for Solar Energy Systems ISE, Department of Energy Systems, Heidenhofstrasse 2, 79110 Freiburg, Germany
[b] Department of Chemical Engineering, University of South Carolina, Columbia, USA

ARTICLE INFO

Article history:
Received 14 November 2007
Received in revised form 27 March 2008
Accepted 30 March 2008
Available online 26 April 2008

Keywords:
Direct methanol fuel cell
Passive operation
Vapor-fed
Characterization
Micro-structuring

ABSTRACT

The impact of structural parameters and operating conditions has not been researched yet for vapor-fed operation of a DMFC at near-ambient conditions. Thus, a detailed parameter study that included reference cell measurements to assess anode and cathode losses separately was performed. Among other parameters like temperature or air stoichiometry, different opening ratios that controlled evaporation of methanol into the vapor chamber were examined.

Water management was found to be a critical parameter for a vapor-fed DMFC. Depletion of water inside the anode catalyst layer, especially at higher current densities, decreased performance of the fuel cell substantially. Back diffusion of water from the cathode to the anode was examined. A micro-structured cathode electrode that increased water back diffusion due to a reduced mass transfer resistance was developed and investigated. Finally, efficiencies and heat losses of a vapor-fed DMFC were determined.

1. Introduction

The portable electronic device market is quickly outgrowing the capabilities of existing batteries. Thus great effort is made to enable fuel cell technology to assist or even replace current battery technology [1,2]. A promising candidate for applications with low power consumption is the micro direct methanol fuel cell (μDMFC), since methanol (MeOH) allows a convenient fuel storage compared to hydrogen. Still some major obstacles have to be overcome toward commercialization of a μ DMFC system.

One of the problems is caused by the formation of CO_2 during the methanol oxidation reaction (MOR), leading to a two-phase flow of the liquid fuel and the gaseous CO_2 within the anode. The gas bubbles may block parts of the catalyst-coated membrane (CCM), become immobile and even block channels completely, a problem that is well known in microfluidics [3]. Therefore, MeOH is typically supplied by a continuous flow using micropumps to force bubbles and dissolved CO_2 out of the anode compartment. However, micropumps typically have a low efficiency [4] and consume a non-negligible amount of the energy produced by the fuel cell.

Two-phase problems, like CO_2 bubble removal, can be avoided if MeOH is delivered in the vapor phase to the anode electrode. The first papers on vapor-fed DMFCs (VDMFC), which were published in the 1990s, reported using a vaporizer at high temperatures between 130 and 200 ° C [5–7]. The fuel cell itself was kept well above the boiling point of MeOH at around 100 °C. Hogarth et al. [7] stated that the performance of their vapor-fed system exceeded by some margin performance of their liquid-fed systems. Power densities up to 0.22 W/cm^2 using air at the cathode were achieved. The impedance of VDMFCs has been studied by Fukunaga et al. [8] and Furukawa et al. [9]. Kallo et al. [10] found that membrane conductivity is an important parameter for a VDMFC and that MeOH crossover is lowered for vapor-phase operation and decreases with increasing temperature. He also studied the transient behavior of a VDMFC [11].

Vapor-phase operation at high temperatures is incompatible with the need for passive approaches for portable DMFCs. In addition, the vaporizer has a high energy consumption, and thus decreases the system efficiency. Recently, much has been published on MeOH mass transfer resistances at the anode, e.g. by using a microporous plate, to lessen the impact of MeOH crossover for liquid-fed DMFCs (LDMFC) [12–14]. Kim et al. [15] used hydrogels in a MeOH fuel cartridge as a diffusion-rate-controlling agent that suppressed MeOH crossover in passively operated LDMFCs. Although they did not specify vapor-phase operation, probably most of the liquid MeOH that had soaked into the hydrogel they used during their experiments was in vapor–liquid equilibrium

Abbreviations: ACL, anode catalyst layer; CCL, cathode catalyst layer; CCM, catalyst-coated membrane; DMFC, direct methanol fuel cell; GDL, gas diffusion layer; LDMFC, liquid-fed direct methanol fuel cell; MeOH, methanol; MOR, methanol oxidation reaction; MPP, maximum power point; RHE, reversible hydrogen electrode; OCV, open circuit voltage; ORR, oxygen reduction reaction; PDMS, polydimethyl siloxane; PTFE, polytetrafluorethylene; VDMFC, vapor-fed direct methanol fuel cell.

* Corresponding author. Tel.: +49 7544 6209.
E-mail address: steffen.eccarius@gmx.de (S. Eccarius).
URL: http://www.ise.fraunhofer.de (S. Eccarius).

0378-7753/$ – see front matter © 2008 Elsevier B.V. All rights reserved.
doi:10.1016/j.jpowsour.2008.03.091

Nomenclature

an	anode
ca	cathode
ohm	ohmic
ref	reference
η	efficiency (%)
ΔG	Gibbs free energy change (kJ mol^{-1})
ΔH	Enthalpy change (kJ mol^{-1})
F	Faraday constant (9.648 × 10^4 C mol^{-1})
i_{leak}	leakage current density (A cm^{-2})
I	cell current (A)
n	amount of substance (mol)
q	heat flux density (W cm^{-2})
R	resistance
U	voltage (V)

inside the anode chamber, as similar open circuit voltages (OCV) for the 4 and 8 M MeOH solution indicate.

Thermodynamically driven evaporation of MeOH at ambient temperatures was utilized for this work. Instead of hydrogels, membranes were used as phase barriers between the liquid and the gaseous MeOH. Usually phase separation membranes are used to separate mixtures of liquids by partial vaporization through the dense membrane, a process called pervaporation [16]. One side is kept at ambient pressures while the other side is under vacuum to increase the driving force, the chemical potential difference. For the vapor-phase operation, these membranes were used as an evaporator under ambient conditions. The chemical potential difference in this case was created by consumption of MeOH during the anodic MOR that disturbed the thermodynamic equilibrium and forced MeOH to diffuse from the storage tank into the anode chamber. Just recently similar concepts have been published by Kim [17] and Guo et al. [18,19].

2. Experimental

2.1. CCM preparation

Nafion®was used as the ionomer for the CCMs. During pretreatment of the membranes, a tempering step was performed at 150 ◦ C for 30 min. DMFC membranes were screen printed on an EKRA E1 semi-automatic screen printer, equipped with a screen having the working electrode and reference electrode design. The anode side of the membrane was printed two, three or four times, depending on the loading required, using a screen-printing paste based on PtRu black and Nafion® ionomer. After drying overnight, the anode loading was determined gravimetrically. The cathode side was printed with the same procedure, using an electrode paste based on high surface-area, carbon-supported Pt and Nafion® ionomer. After drying for another night, the loading of the cathode was determined.

For post-treatment of the CCMs, the air-dried CCMs were tempered at 145 ◦ C for 30 min and slowly cooled down. After tempering, the CCMs were placed in boiling 5 wt% nitric acid for 30 min, then placed in boiling deionized water twice for 30 min each, and after cooling down put in cold water, also for 30 min. The CCMs were then dried between lint-free paper, pressed between wooden plates. Unless stated otherwise in the text CCMs of Nafion® 1135 that had been screen-printed three-times with Johnson Matthey's HiSPEC11100 (resulting in 1 mg cm^{-2} Pt) at the cathode electrode and that had been screen-printed three-times with Johnson Matthey's HiSPEC6000 (resulting in 3 mg cm^{-2} Pt/Ru) at the anode electrode, were used. The reference electrodes had the same composition as the respective electrode, i.e. working anode or cathode, on the same side of the membrane.

After preparation of the CCMs, a postprocessing method using a laser ablation of the catalyst layer was applied. This guaranteed small measurement errors in using the attached reference electrode and is described in detail in [20].

2.2. Fuel cell assembly

The design of the evaporator and the anode that were used throughout vapor-phase operation experiments is shown in Fig. 1. Liquid MeOH was stored in a temperature-controlled storage tank and a needle valve was used to equalize the pressure between the tank and the surroundings. A plate of FR-4, a material used for making printed circuit boards, was used to change opening ratios. The opening ratio is defined as the open area versus the total area of the plate. The plate and the phase separation membrane were attached between VITON sealing rings. The gold plated, stainless steel anode plate was used to give mechanical strength as well as to collect current, having a 1 mm breached serpentine structure. Vaporized MeOH diffused into the anodic vapor chamber and was oxidized at the anode catalyst layer (ACL). Atmospheric pressure was maintained through an outlet, where in particular CO_2could leave the vapor chamber.

Cathode plates were constructed from a graphite compound material with both the working electrode flowfield and the isolated reference electrode flowfield (milled 0.8 mm into the material). A serpentine flowfield with 1 mm wide channels was chosen. Connectors allowing direct measurement of the voltage without measuring at the current collectors were attached to the graphite material. A thermo-couple was placed directly at the center of the working electrode on the back of each cathode. The working electrode had an area of 10 cm^2. The reference electrode, which was offset 30 mm to one side of the working electrode, had an area of 1 cm^{2}and a 1 mm serpentine flowfield. The large distance between the working electrode and the reference electrode was chosen to guarantee that no MeOH could diffuse in-plane between the working and the reference electrode. If MeOH diffuses from the working anode electrode to the reference electrode the reference potential of the reversible hydrogen electrode (RHE) could change during operation, leading to additional errors in the measurement [20].

2.3. Measurement and operation

In addition to an initial treatment of new MEAs, the fuel cell was preconditioned before each experiment. Therefore, the cell voltage was cycled four times from 0.6 V down to 0.05 V and up to 0.6 V again in 50 mV steps, each step lasting 10 s. This procedure was repeated if a strong hysteresis was detected between the third and fourth cycle.

Polarization measurements started at the OCV. The voltage was decreased in 25 mV-steps to short circuit or voltages slightly above short circuit with each step lasting 20 s. This measurement was repeated in order to study if hysteresis effects were present. The actual ohmic cell resistance was obtained using a Milliohmmeter which recorded the real part of the impedance at 1 kHz. It summarizes all ohmic losses R_{ohm} like flowfield resistances, contact resistances, membrane resistances etc. Thus the IR-free anode losses η_{an} and cathode losses η_{ca} could be calculated using the potential between the attached RHE and the anode/cathode electrode:

$$\eta_{an} = U_{ref-an} - \frac{R_{Ohm} I}{2} \quad (1)$$

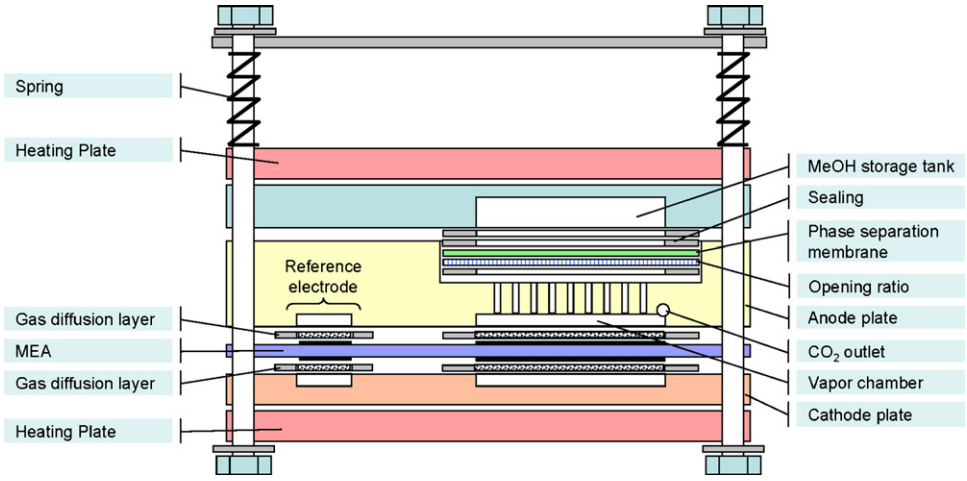

Fig. 1. Test cell used for experiments with the vapor-fed DMFC. Liquid MeOH is stored in the tank and is evaporated into the vapor chamber using the phase separation membrane. The vapor chamber has one outlet to release CO_2 into the atmosphere.

$$\eta_{ca} = U_{ref-ca} - \frac{R_{Ohm} I}{2} \quad (2)$$

Here, U_{ref-an} stands for the potential of the anode versus the RHE whereas U_{ref-an} stands for the potential of the cathode versus the RHE. Because of a homogeneous potential distribution within the membrane the deduction of half of the ohmic losses was justified [20].

Crossover measurements were performed by sampling the cathode exit gas each second using a mass spectrometer (*MKS Mini-Lab*). Before the experiments started, the mass spectrometer was calibrated with gas mixtures similar to those expected. Compressed air was analyzed in order to get the baseline for differential measurements.

The CO_2crossover from the anode to the cathode was determined in half-cell operation of the DMFC [21]. During half-cell experiments, the cell was potentiostated with hydrogen supplied to the cathode at a flow rate of 15 sccm. The absence of oxygen prevented methanol on the cathode side from being oxidized. For this case, all of the CO_2measured in the cathode outlet stream must have crossed the membrane from the anode.

In full-cell operation, air or oxygen is provided to the cathode electrode. In addition to CO_2crossing over from the anode, CO_2 is formed by the parasitic oxidation of methanol at the cathode. If not all of the methanol is oxidized inside the CCL, methanol should be present inside the cathode flowfield. Thus both the CO_2 and the methanol concentrations were measured inside the cathode outlet stream during functional DMFC operation. An equivalent current was calculated from the mass flow for better comparison to the cell current:

$$I_{leakage} = \frac{N_{MeOH,ca}}{6F} \quad (3)$$

Faraday's law is applied to calculate the leakage current $I_{leakage}$. Electrochemical oxidation of MeOH as a 6-electron transfer process is assumed. Vielstich et al. [22] suggested that parallel chemical oxidation of MeOH occurs at high cathode potentials (>0.5 V versus RHE). Nevertheless for simplicity Eq. (3) is commonly used in the literature [23,24].

3. Results and discussion

3.1. Parameter study

The impact of operating conditions and structural parameters on the performance as well as on polarization and concentration losses of a VDMFC was studied. The connected RHE was used to assess losses individually. A PDMS membrane at an opening ratio of 6.8% was used to evaporate a 50 wt% solution of MeOH in deionized water into the vapor chamber. Dry air was supplied to the cathode flow channel. A minimum air flow rate of 40 sccm was set before switching to a stoichiometry of 2 at a current density of 0.11 A cm^{-2}. Hydrogen, which was humidified inside a washing bottle at ambient conditions, was fed to one electrode of the RHE. The other electrode of the RHE was flooded with deionized water to guarantee a stable reference potential. The temperature of the cell was kept constant at 50 °C. A 300 μm thick, non-teflonized GDL was used on both the anode and the cathode side. For the CCM, Nafion®1135 being screenprinted with HiSPEC 6000 (3 mg cm^{-2} Pt/Ru) at the anode and HiSPEC 11100 (1 mg cm^{-2} Pt) at the cathode was used. The clamping force on the cell was set to 3450 N, which results in a pressure of 345 kPa on the GDL. These standard conditions were applied unless stated otherwise in the text.

3.1.1. Structural parameters of the MEA

The influence of two different membrane thicknesses and catalyst loadings on the electric properties of the VDMFC were studied. Besides the commonly used Nafion® 117, which had a high Pt/Ru catalyst loading of 3 mg cm^{-2} at the anode electrode for this work and provided low crossover at sufficiently high current densities, thinner Nafion® 1135 and low anode loadings of 1 mg cm^{-2} were also studied.

The following CCMs were investigated:

- Nafion® 117 screen-printed three times using HiSPEC 11100 at the cathode electrode (equal to 1 mg cm^{-2} Pt) and three times using HiSPEC 6000 at the anode electrode (equal to 3 mg cm^{-2} Pt/Ru).
- Nafion® 117 screen-printed three times using HiSPEC 11100 at the cathode electrode (equal to 1 mg cm^{-2} Pt) and once using HiSPEC 6000 at the anode electrode (equal to 1 mg cm^{-2} Pt/Ru).
- Nafion® 1135 screen-printed three times using HiSPEC 11100 at the cathode electrode (equal to 1 mg cm^{-2} Pt) and three times

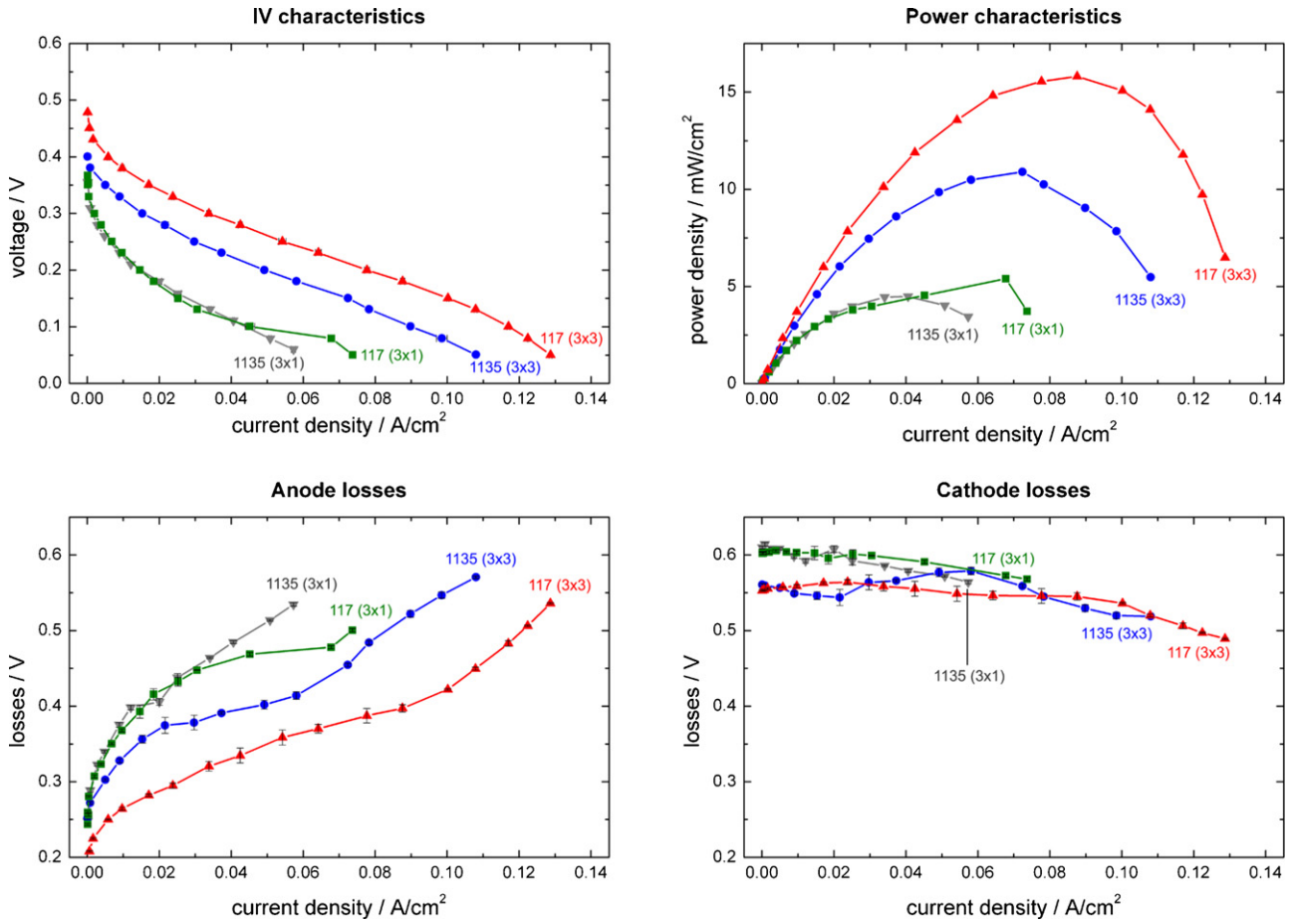

Fig. 2. Electric properties of a VDMFC for different membranes and catalyst loadings. Anode and cathode polarization losses were calculated using a connected reference RHE. The temperature was 50 °C, the cathode air stream 40 sccm/ λ 6, the evaporator opening ratio 6.8% and MeOH concentration 75 wt%.

using HiSPEC 6000 at the anode electrode (equal to 3 mg cm^{-2} Pt/Ru).

- Nafion® 1135 screen-printed three times using HiSPEC 11100 at the cathode electrode (equal to 1 mg cm^{-2} Pt) and once using HiSPEC 6000 at the anode electrode (equal to 1 mg cm^{-2} Pt/Ru).

Results of this characterization can be found in Fig. 2. It is obvious that the CCMs having a high anode catalyst loading outperformed the others. It can also be observed that Nafion®117 had a slightly better performance compared to the thinner Nafion®1135. Looking at the individual electrode polarization losses, it is interesting to note that the thickness of the membrane did not seem to affect cathode losses, which reflected MeOH crossover among other effects. This is especially obvious at OCV, when no MeOH was consumed at the ACL and the electroosmotic drag vanished. The catalyst loading at the anode had a much higher impact on the crossover as the thicker anode electrode offered a higher mass transfer resistance to the MeOH. Besides these effects, better anode performance at high catalyst loadings is displayed.

The different IV characteristics between the two membranes were caused on the anode side. Nafion® 117 displayed lower anode losses. This is surprising as back diffusion of product water from the cathode, which greatly influences anode performance as will be shown later, should be higher at thinner membranes. Apparently water transport was enhanced by Nafion® 117, especially at higher current densities.

3.1.2. *Methanol concentration*

Experiments with different MeOH solutions in deionized water at 25, 50 and 75 wt% and pure MeOH were conducted to study the impact of MeOH concentration on a VDMFC. All other operational and structural parameters were kept constant.

The IV characteristics and the electrode losses are depicted in Fig. 3. It should be mentioned that these results are valid only for an opening ratio of the evaporator of 6.8% and will change when the opening ratio is varied. Optimal performance for the given conditions was achieved by having a 50 wt% solution of MeOH; it decreased for higher and lower concentrations. Two opposing effects could be studied on the anode and the cathode. Crossover increased with MeOH concentration and consequently cathode losses increased as shown. The great difference between pure MeOH and the three solutions indicated a much higher crossover, probably combined with partial flooding of the cathode.

Anode losses decreased as expected with increasing MeOH concentration. Besides having higher partial pressures of MeOH at the anode electrode, resulting in higher anodic current densities, the water concentration at the anode also greatly influenced the electrode losses. According to the Antoine equation with parameters for MeOH and water, the amount of evaporated water is only a fraction of the evaporated MeOH, depending on the MeOH concentration. Because one mole of water is needed to oxidize one mole of MeOH, the lack of water is slowing down the MOR.

As already mentioned, high MeOH concentrations result in a high crossover rate. Usually most of this cathodic MeOH is oxidized

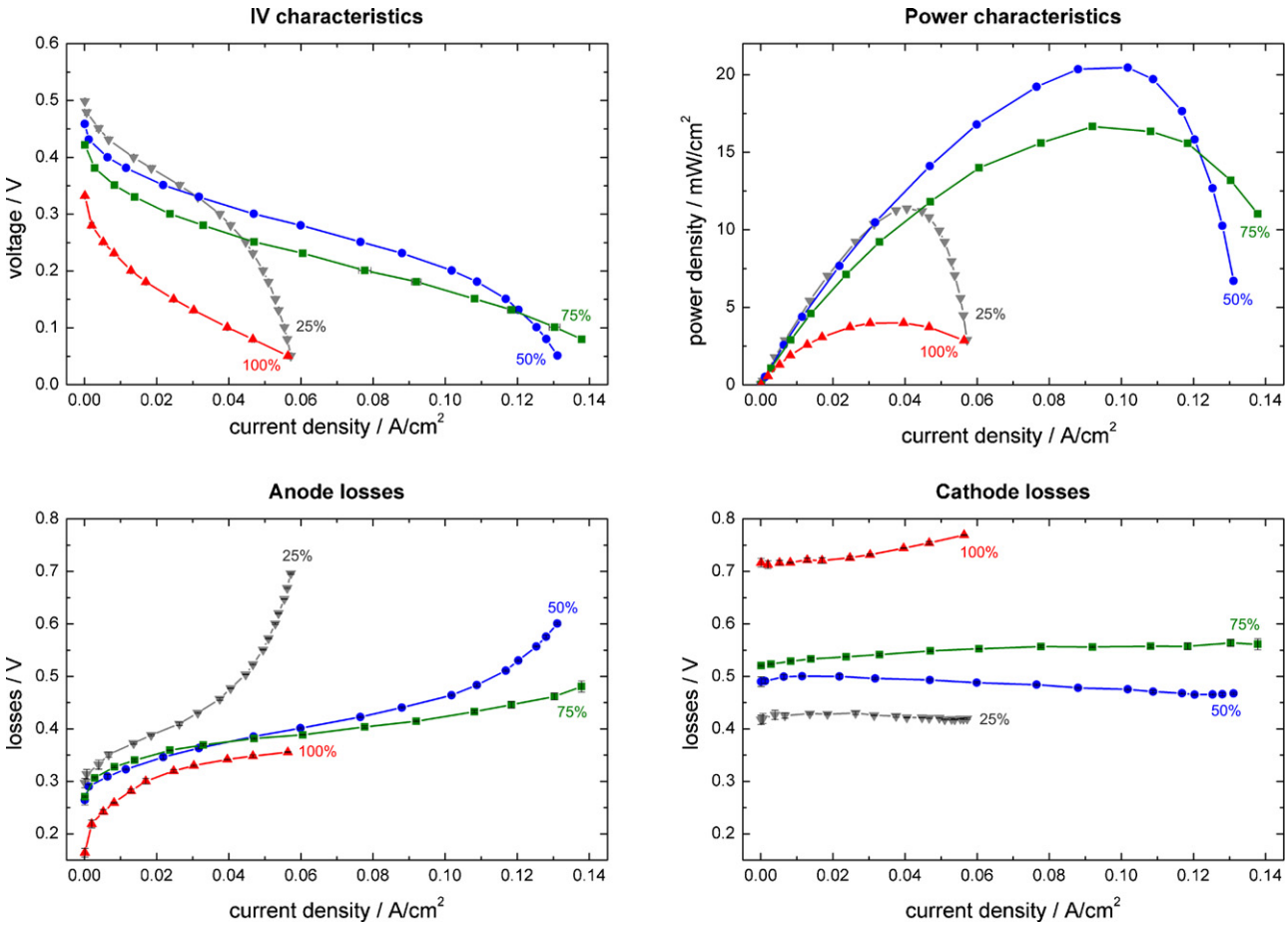

Fig. 3. Electric properties of a VDMFC for different MeOH concentrations. Anode and cathode polarization losses were calculated using a connected reference RHE. The temperature was 50 °C, the cathode air stream 40 sccm/ λ 2 and the evaporator opening ratio 6.8%.

to CO_2 and water. Thus, the water concentration at the cathode increases with crossover and back diffusion of water to the anode is enforced because of a large concentration gradient between the anode and the cathode. The assumption is validated by the electrode losses of pure MeOH, where high cathode losses indicate high crossover and thus high water concentration that hinders oxygen access to the cathode catalyst layer (CCL). The anode electrode for pure MeOH performed slightly better than at 50 and 75 wt% and much better than at 25 wt%.

This conclusion was supported by examining the ohmic high frequency resistances at 1 kHz for all cases, as shown in Fig. 4. The membrane resistance is a major part of the overall ohmic resistance, which therefore strongly correlates with the water content of the membrane. The ohmic resistance decreases with increasing water saturation of the ionomer [25] and thus reveals information about the humidification of the membrane. It can be noted that for a 25 wt% solution of MeOH, the resistance was much higher than for pure MeOH. This clearly indicated less water saturation inside the ionomer at lower MeOH concentrations due to lower crossover. Therefore, the water concentration at the cathode and back diffusion of water to the anode was reduced as well. Effects of these mass transport problems could be seen in the anode losses. For pure MeOH, the membrane resistance was only slightly smaller than for 75 wt%, and it can be concluded that product water at the cathode was no longer uptaken significantly by the ionomer. Thus flooding at the cathode, reflected by high cathode losses, occurred and water back diffusion to the anode increased, lowering the anode losses.

3.1.3. Cathode stoichiometry

The cathode flow rate was varied during this parameter study. Air was forced through the cathode flowfield at stoichiometries of 2, 4 and 6 with a minimum flowrate of 40 sccm.

Results of this study can be seen in Fig. 5. A sharp drop at higher current densities indicating high concentration losses was found in the IV plots for all stoichiometries. Surprisingly the performance

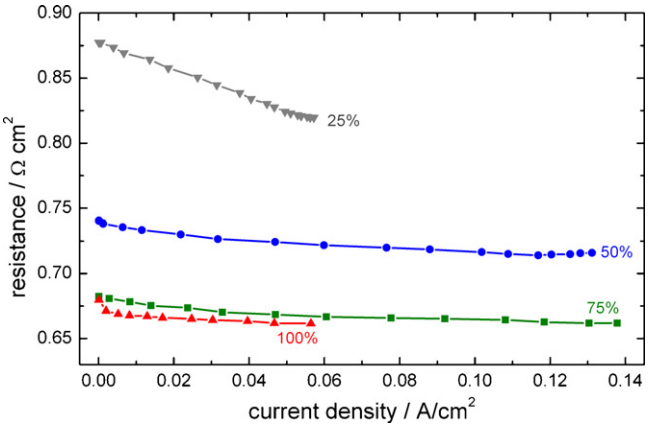

Fig. 4. Ohmic resistance of the VDMFC versus current density. The temperature was 50 °C, the cathode air stream 40 sccm/ λ 2 and the evaporator opening ratio 6.8%. The MeOH concentration in the storage tank was varied.

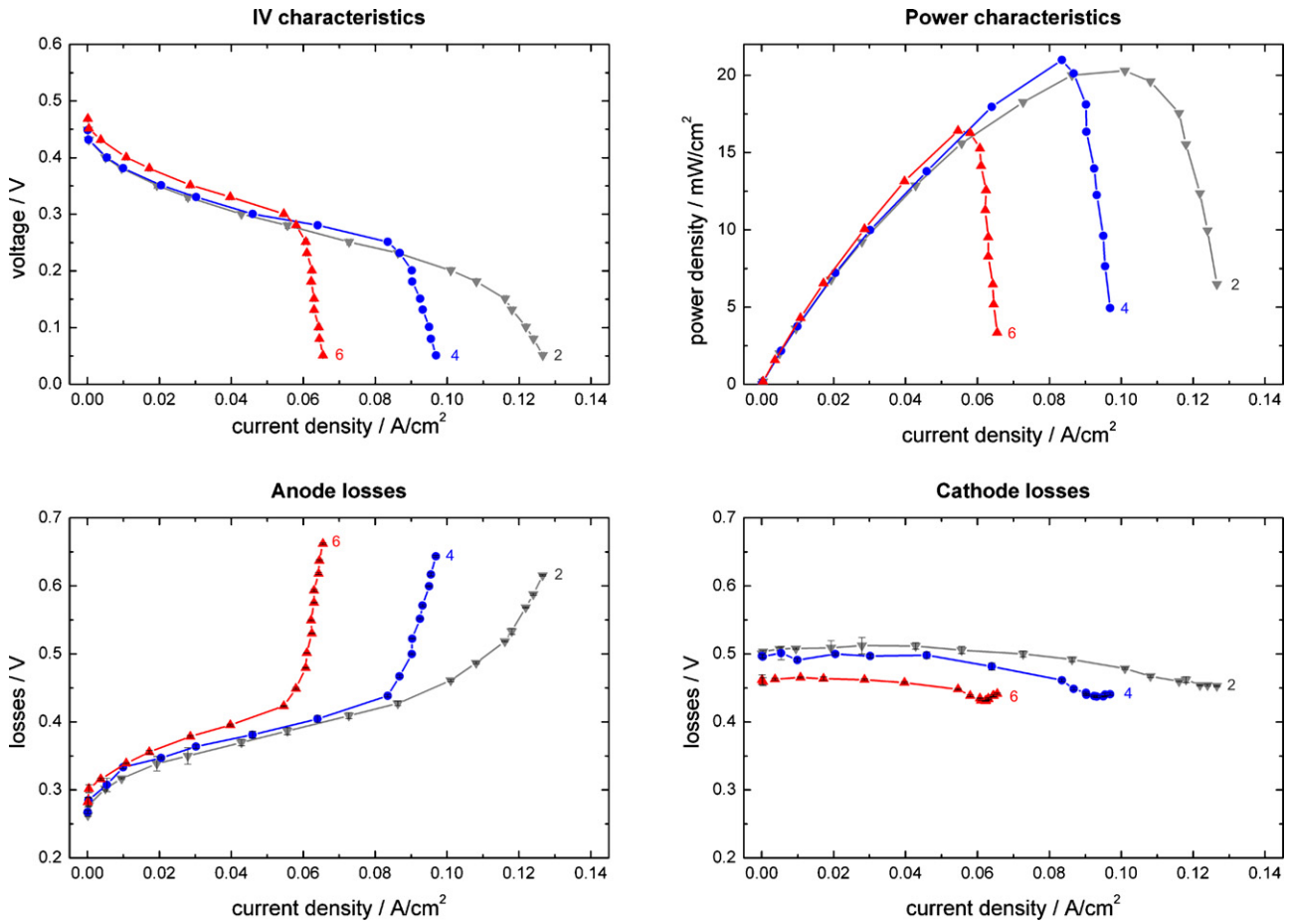

Fig. 5. Electric properties of a VDMFC for different cathode air stoichiometries. Anode and cathode polarization losses were calculated using a connected reference RHE. The temperature was 50 °C, the minimum cathode air stream was 40 sccm and the evaporator opening ratio 6.8%.

of the VDMFC declines with increasing air flow rate. For liquid-fed DMFCs, the performance increases when the cathode stoichiometry is increased [26,27]. Here flooding can be prevented at higher stoichiometries and the impact of the parasitic MeOH oxidation at the cathode electrode can be reduced because of higher oxygen partial pressures. Lower cathode losses at higher flow rates were also found for the VDMFC, having the same cause as in the liquid-fed case.

The reason for the sharp drop in the IV curve could be found at the anode electrode. The maximum current density decreased from 130 mA cm^{-2}at an air stoichiometry of 2 to only 60 mA cm^{-2} at an air stoichiometry of 6. The sharp drop of the anode losses further implied limited access to one of the reactants of the MOR. As the evaporation of MeOH was not changed in this series of experiments the water concentration within the anode and thus the limiting current densities were changed at different stoichiometries. At lower cathode flow rates, less product water could be transported away from the cathode. The concentration gradient between the cathode and the anode increased as most water molecules at the anode were consumed during the MOR. Thus, back diffusion of water to the anode increased at lower stoichiometries.

3.1.4. Temperature

The large thermal masses of the test cell that could be thermostatted externally allowed isothermal operation of the VDMFC. The impact of temperature was studied at 30, 50 and 70 ° C and results are shown in Fig. 6. The performance of liquid-fed DMFCs increases with temperature [27–31]. For the VDMFC, the performance increased significantly between 30 and 50 ° C and then stayed stable, reaching an maximum power point (MPP) of 20 mW/cm^2, whereas the limiting current density increased further. The cause therefore could again be found at the cathode electrode. Higher temperatures facilitate crossover, which – depending on operation conditions and structural parameters – can also be found for liquid-fed DMFCs [32], and thus yield increased cathode losses. Conversely, higher crossover increases water production at the cathode and back diffusion of water to the anode electrode is enhanced.

Temperature influenced several effects on the anode side that can be noticed in the anode losses. First, more MeOH was evaporated from the liquid reservoir at higher temperatures. The partial pressure of MeOH at the anode increased, causing a higher current production. Second, MeOH oxidation is a highly temperature-dependent reaction, especially in the given temperature range. This is also known for diluted MeOH in LDMFCs. Here, the anode losses were significantly decreased going from 30 to 50 ° C so that the limiting current density could be doubled. This effect holds true for the VDMFC as well and the limiting current density could be tripled. Third, higher back diffusion of water from the cathode improves the kinetics of the MOR. This is apparent at 30 and 50 ° C where a steep rise of the anode losses close to limiting current occurs, which cannot be seen at 70 °C.

3.1.5. Gas diffusion layer

300 μm thick GDLs were used at different PTFE loadings with and without a microporous layer. Adding PTFE increases the

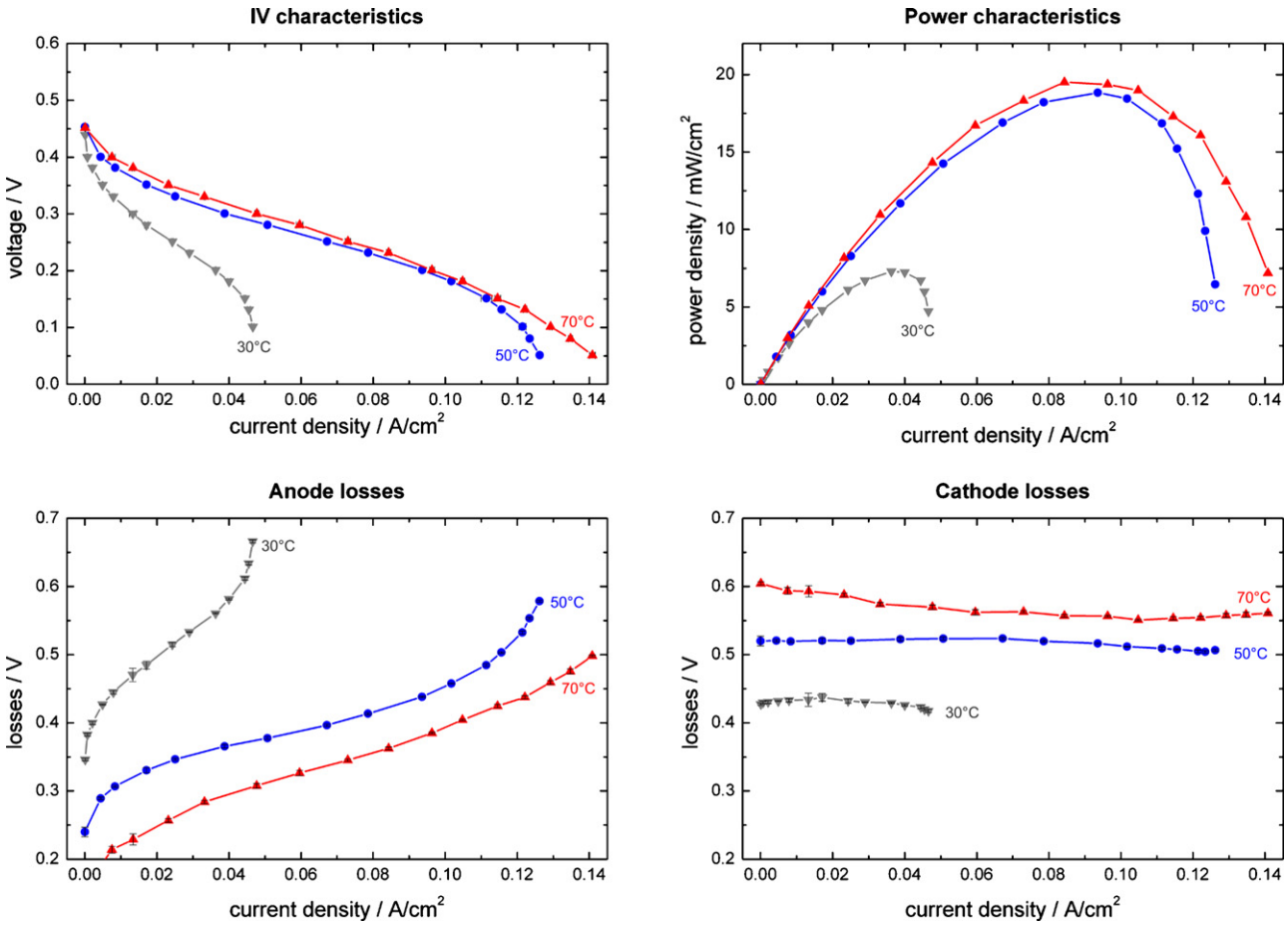

Fig. 6. Electric properties of a VDMFC for different temperatures. Anode and cathode polarization losses were calculated using a connected reference RHE. The cathode air stream was 40 sccm/ λ 2 and the evaporator opening ratio was 6.8%.

hydrophobicity of the material. Four different GDLs were prepared and each was studied for both the anode and the cathode at the same time:

- GDL 35 AA (not modified),
- GDL 35 BA (5 wt% PTFE),
- GDL 35 BC (5 wt% PTFE including a microporous layer) and
- GDL 35 DC (20 wt% PTFE including a microporous layer).

Experimental results for this study are shown in Fig. 7. The performance for all GDLs under investigation was quite similar. Significant deviations could be seen only close to limiting current density. The cathode losses were least when the unmodified GDL was mounted on both sides. Treatment of the GDL with PTFE slightly decreases pore sizes and hydrophobizes the material. Therefore, oxygen access to the three-phase boundary of the catalyst layer is expected to be highest for unmodified GDLs when no flooding is present, which was supported by the low cathode losses. A microporous layer on the cathode does not seem to influence cathode losses considerably.

On the anode, a large difference between GDL 35 BA without and 35 BC with a microporous layer can be noticed. The limiting current density was increased by 40 mA cm^{-2}without the microporous layer. Similar behavior occurred for unmodified GDLs and hydrophobized GDLs having 5 wt% of PTFE. For unmodified GDLs, large amounts of product water could leave the cathode electrode, reducing back diffusion to the anode. A lack of water at the anode caused high concentration losses at high current densities. Hydrophobic GDLs improved the back diffusion of water, as can be seen for GDL 35 BA. The microporous layer that caused slightly lower anode losses at low current densities exhibited high concentration losses at higher current densities. Transport of MeOH to the anode electrode was probably limited by the higher mass transfer resistance of the microporous layer, reducing current generation.

3.1.6. Evaporator opening ratio

The concentration of MeOH inside the vapor chamber at different current densities is inherently coupled with geometric and material properties of the evaporator as well as with MeOH concentration in the storage tank. Inlays with five different opening ratios of 1.7, 3.4, 6.8, 13.6 and 27.2% were manufactured to study the influence of the opening ratio. Four different MeOH solutions of 25, 50 and 75 wt% in deionized water and pure MeOH were used throughout the epxeriments. Nafion® 117 was used as membrane throughout these experiments.

The dependence of anode and cathode losses of the fuel cell on three different opening ratios of 1.7, 3.4 and 27.2% at a MeOH concentration of 25 and 100 wt% is illustrated in Fig. 8. Two different behaviors at the two MeOH concentrations can be noted. Anode losses for the 25 wt% MeOH solution decreased with increasing opening ratio. This behavior can be attributed to concentration losses of MeOH and water at the anode electrode. Cathode losses increased with increasing opening ratios. Therefore, MeOH concentration in the vapor chamber and consequently MeOH crossover from anode to cathode increased at higher opening ratios, a fact that will be discussed later in this paper. Water production at the cath-

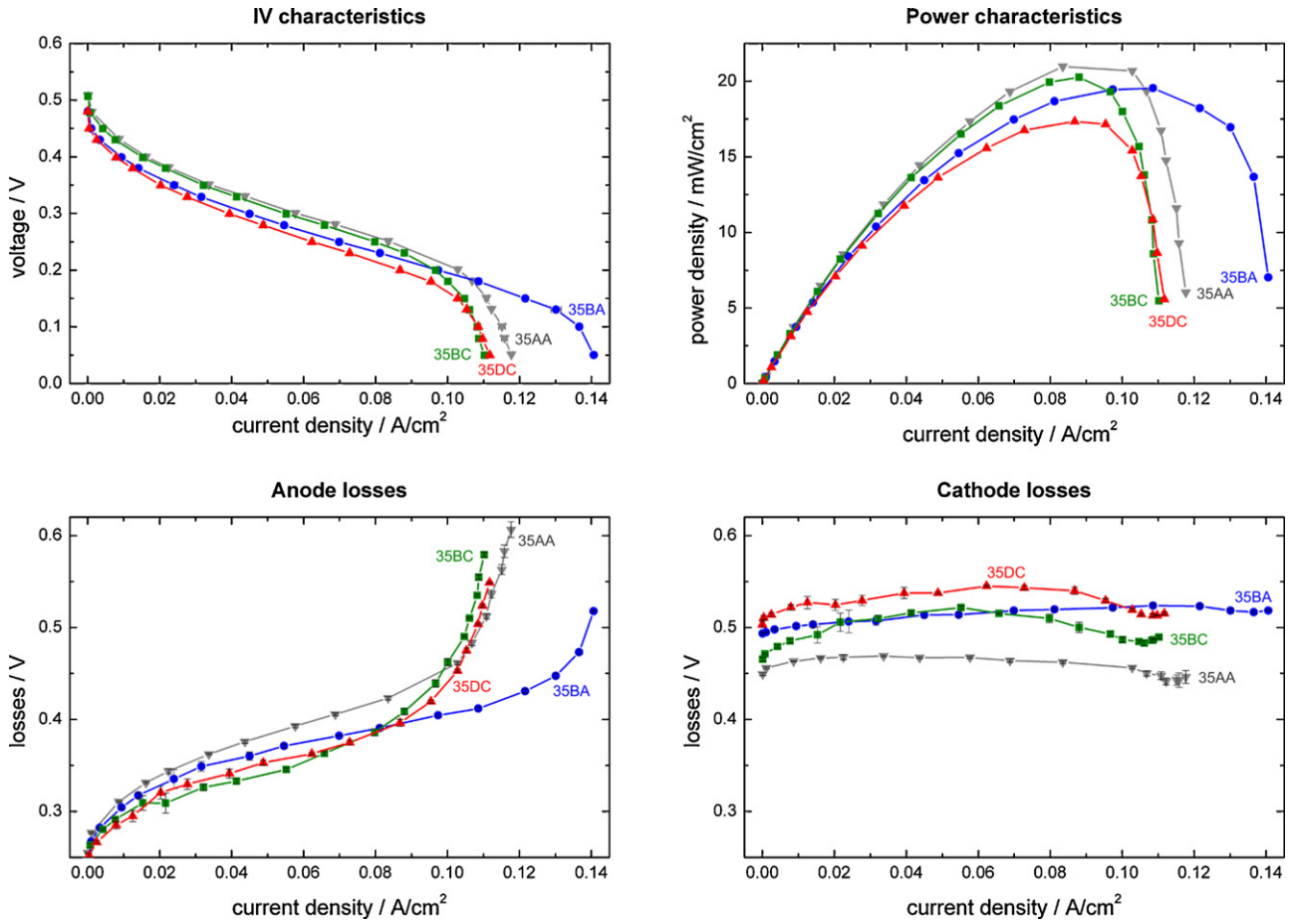

Fig. 7. Electric properties of a VDMFC for different GDL parameters. Anode and cathode polarization losses were calculated using a connected reference RHE. The temperature was 50 °C, the cathode air stream 40 sccm/ λ 2 and the evaporator opening ratio 6.8%.

ode electrode was facilitated at higher leakage currents and water back diffusion to the anode increased, which minimized water concentration losses of the MOR.

Anode losses for the 100 wt% MeOH solution did not change significantly with different opening ratios except close to limiting current density for an opening ratio of 1.7% where concentration losses occured. Polarization losses for this opening ratio were similar to polarization losses of the 25 wt% MeOH solution at 27.2% opening ratio, which reckoned same partial pressures of MeOH within the vapor chamber. Cathode losses at the highest opening ratio were extremly large at values of 750 mV versus RHE, indicating large flooded areas because of a high MeOH crossover.

It can be concluded from the figures that MeOH crossover increased with opening ratio as well as with MeOH concentration. Partial pressures of MeOH in the vapor chamber increases with MeOH concentration. At high partial pressures the concentration gradient of MeOH between anode and cathode rose and crossover was enlarged.

The complex interaction between opening ratio and MeOH concentration on the limiting current density is depicted in Fig. 9. The partial pressure of water and MeOH in the vapor chamber, which influenced MeOH crossover to the cathode and water back diffusion from the cathode, greatly affected the maximal current density. It is interesting to note that the current densities that were achieved exceeded the maximal current densities that could be achieved when multiplying the opening ratio to the evaporative flux for a dense membrane at 50 ° C (the active area of the fuel cell equaled the active area of the evaporator). The values determined by Beard et al. were multiplied by the opening ratio and introduced in Fig. 9 as a dotted line. Thus it is not evaporation, but diffusion or adsorption in the dense membrane that was the rate limiting step for the mass transport. The relation between opening ratio and evaporative flux into the vapor chamber is not necessarily linear as it depends e.g. on geometric properties of the opening ratio plate.

3.2. Methanol crossover

The driving force for MeOH crossover from the anode to the cathode side across the membrane differs between liquid-fed and vapor-fed operation of a DMFC. While diffusion due to a concentration gradient between the anode and cathode is the major mechanism for VDMFCs, contributions of the electroosmotic drag are significant and cannot be neglected for LDMFCs [32]. Additionally, MeOH crossover is much smaller for the VDMFC, a fact also found by Kallo et al. [10].

Leakage current densities at 50 ° C for a LDMFC and two MeOH concentrations of 0.5 M and 1.5 M are compared to a VDMFC at 25 and 75 wt% in Fig. 10 along with the respective power densities. It should be noted that the MeOH feed concentration for the VDMFC was much higher (e.g. 75 wt% ≙19.5 M and 1.5 M ≙5 wt%). Further structural parameters and operating conditions are given in Table 1.

The different behavior of the leakage current densities between vapor-fed operation and liquid-fed operation is apparent in the graph. The MeOH crossover decreased linearly for the VDMFC with increasing cell current density. The linear decrease can be attributed to two effects. First, the MeOH concentration inside the

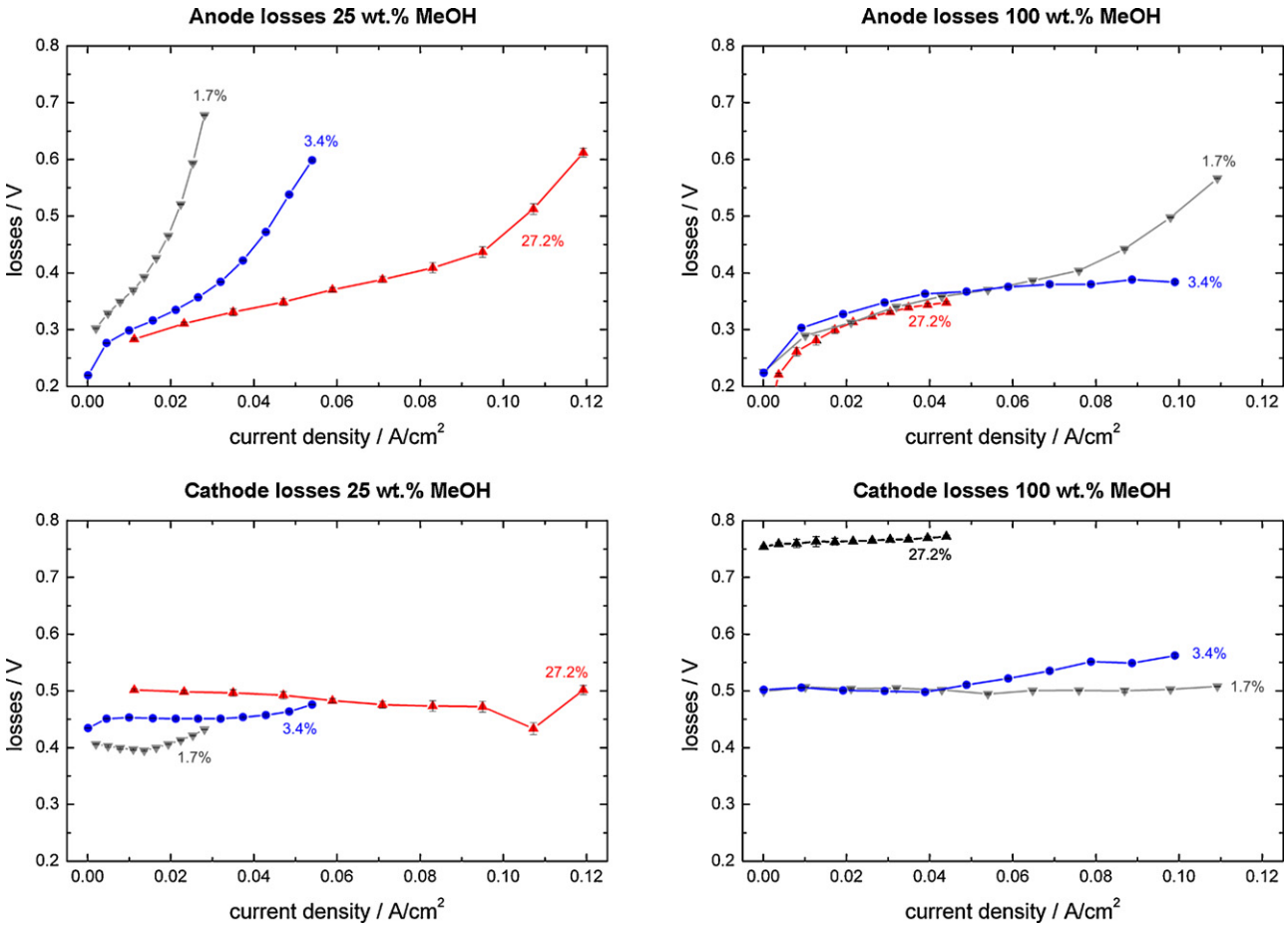

Fig. 8. Anode losses and cathode losses of a VDMFC for different MeOH concentrations and evaporator opening ratios. Anode and cathode losses were calculated using a connected reference RHE. The temperature was 50 ° C and the cathode air stream 40 sccm/ λ 2.

ACL decreases with current density, as more MeOH is needed for the anodic MOR. Second, humidification of the membrane was lowered at higher current densities due to the high consumption of water at the anode electrode. It is a valid assumption that MeOH crossover decreases due to a decreased amount of water in the membrane [10]. For the LDMFC, the contribution of the electroosmotic drag changed the slope of the leakage current density and rose with cell current density. At a MeOH concentration of 1.5 M, the MeOH crossover increased with cell current density for the LDMFC.

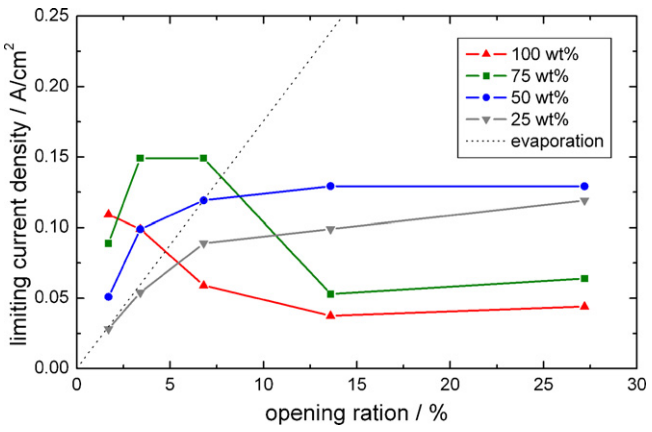

Fig. 9. Influence of different MeOH concentrations and evaporator opening ratios on the limiting current density. The temperature was 50 ° C and the cathode air stream 40 sccm. "Evaporation" is the product of the opening ratio and the evaporative flux for a dense membrane at 50 ° C.

Usually the working point of a DMFC is chosen to be at MPP, which was 0.09 and 0.13 A cm^{-2} for the VDMFC and 0.18 and 0.22 A cm^{-2} for the LDMFC in the given case. MeOH crossover and thus leakage current densities for the LDMFC experiment with a 0.5 M solution of MeOH and air stoichiometry 6 and for the VDMFC experiment with a 25 wt% solution of MeOH and air stoichiometry 2 were similar for the given cell current density at MPP. For the 1.5 M/ λ 6 liquid-fed and the 75 wt%/ λ 2 vapor-fed experiments, the VDMFC had a significantly lower crossover of MeOH at MPP.

In a comparison between liquid-fed and vapor-fed operation, the water uptake of Nafion® is much lower for a VDMFC and crossover of MeOH is reduced, which was also found by Ren et al. [34]. Additionally, the electroosmotic drag plays a minor role for a VDMFC. The evaporative flux of MeOH from a highly concentrated MeOH solution in the storage tank can be controlled by additional mass transfer resistances. As a consequence, MeOH crossover during vapor-phase operation is drastically reduced compared to liquid-phase operation.

It was already mentioned that MeOH crossover was greatly affected by changing opening ratios and MeOH concentrations. Fig. 11 depicts leakage current densities at OCV and 0.04 A cm^{-2}. The leakage current density decreased for all conditions when current was drawn from the cell which indicates that diffusion was the dominating transport process inside the membrane. At larger opening ratios the leakage current density increased due to higher

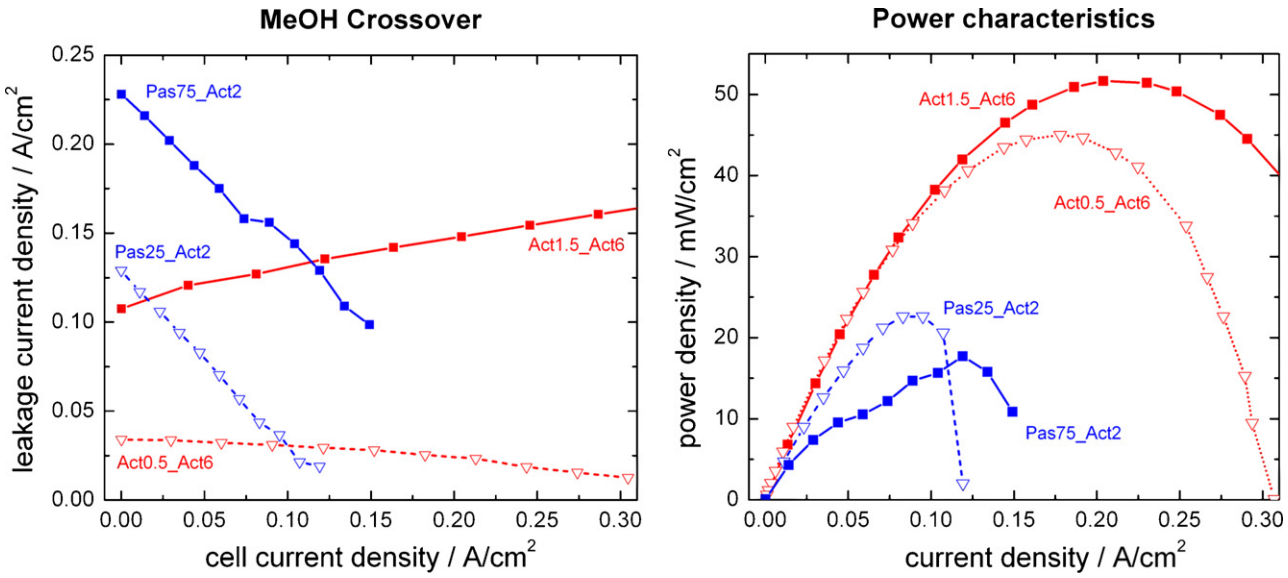

Fig. 10. Leakage current densities and power densities of a LDMFC and a VDMFC for different structural parameters and operating conditions as explained in Table 1. Nafion® 117 was used as the membrane and the temperature was set to 50 °C.

Table 1
Structural parameters and operating conditions of the experiments which differ from the standard conditions as described in the text

Experiment	MeOH concentration	Pump rate (ml min^{-1})	Opening ratio (%)	Stoichiometry
Liquid-fed operation				
Act0.5_Act6	0.5 M	1	-	6 (min 30 sccm)
Act1.5_Act6	0.5 M	3	-	6 (min 30 sccm)
Vapor-fed operation				
Pas25_Act2	25 wt%	-	27.2	2 (min 40 sccm)
Pas75_Act2	75 wt%	-	6.8	2 (min 40 sccm)
Pas100_Act2	100 wt%	-	1.7	2 (min 40 sccm)

MeOH partial pressures in the vapor chamber and thus enlarged the MeOH crossover.

3.3. Water management

One conclusion of the parameter study was that especially at high current densities, fuel cell performance decreased because of a lack of water at the anode electrode. It was shown that high crossover of MeOH led to higher water concentrations at the cathode which increased membrane humidification and decreased membrane resistance. Anode losses close to the limiting current density dropped compared to experiments with lower crossover. A higher back diffusion of water from the cathode to the anode could cope with stoichiometric water consumption during the MOR. As a

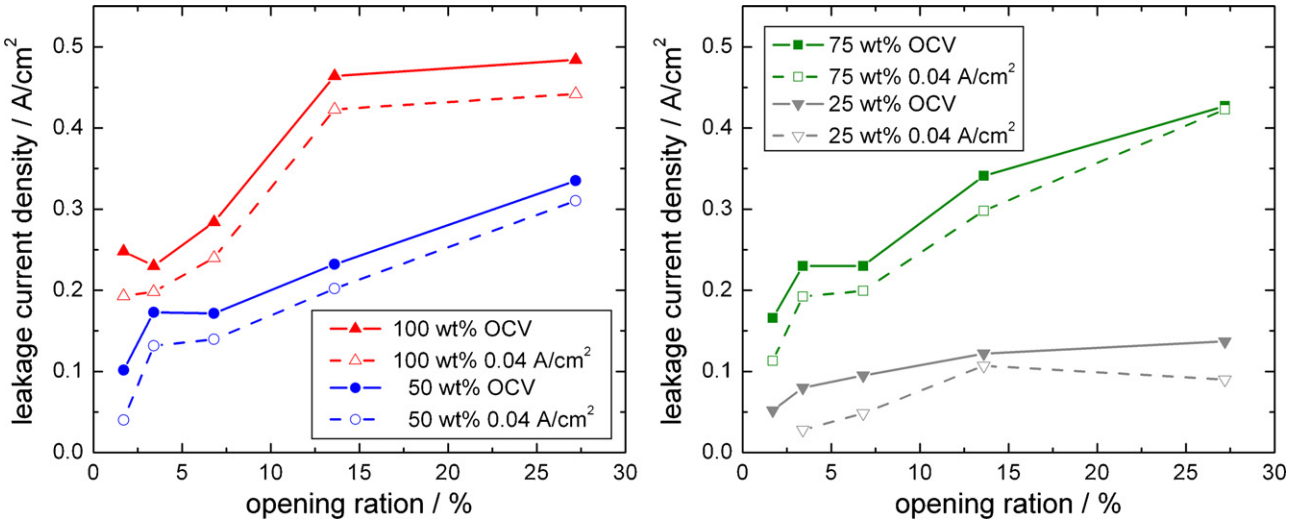

Fig. 11. Influence of different MeOH concentrations and evaporator opening ratios on the MeOH crossover at OCV and 0.04 A cm^{-2}. The temperature was 50 °C and the cathode air stream 40 sccm/ λ 2.

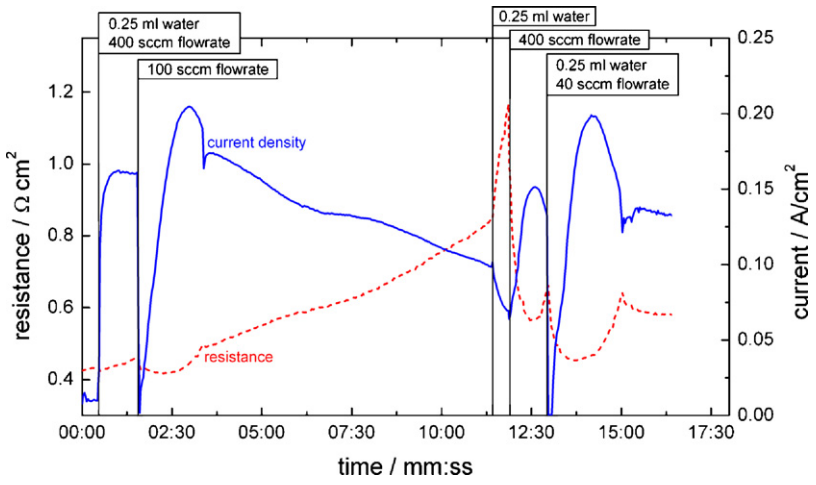

Fig. 12. Influence of several actions to the cathode air stream on the performance and the ohmic resistance of a VDMFC. The cell voltage was kept constant at 250 mV.

consequence, higher water concentrations at the cathode electrode seem to be favorable for a VDMFC.

Elevated crossover of MeOH decreases Faradaic efficiency of the fuel cell and additionally raises the risk of flooding within the pores of the cathode electrode and GDL. Therefore, active supply of water to the cathode electrode was investigated along with a micro-structured cathode electrode that facilitated water back diffusion.

3.3.1. Active supply of water

Performance of a VDMFC at increased cathodic water concentrations was evaluated by actively injecting liquid deionized water into the air supply of the cathode. Most of the conditions from the parameter study Section 3.1 were applied: PDMS membrane with an evaporator opening ratio 6.8%, 50 °C, non-teflonized GDL and changing air flow rates at the cathode. Nafion® 117 with an Pt/Ru anode loading of 3 mg cm^{-2} and a Pt cathode loading of 1 mg cm^{-2} was used instead of Nafion® 1135 because of its better performance. Instead of using 50 wt%, the MeOH concentration was raised to 100 wt%.

The response of the fuel cell to several actions is shown in Fig. 12. The cell voltage was kept constant at 250 mV throughout this experiment. After injecting 0.25 ml of water into an air stream of 400 sccm, the current increased significantly. When the air stream was reduced to 100 sccm, flooding inside the cathode electrode occurred. Flooding decreased after some seconds and current reached its maximum of more than 0.2 A cm^{-2}. Injection of water at 100 sccm caused severe flooding, which was relieved when the flow rate was increased to 400 sccm again. The improvement in performance was also reproducible for lower air flow rates of 40 sccm. The crossover current density responded as expected to cathodic flow rates. It increased with flow rate because more MeOH molecules inside the cathode were consumed during parasitic oxidation. Adding liquid water to the air stream did not have any effect on the crossover current density.

3.3.2. Cathode geometries for increased water back diffusion

The most natural approach to increase the water concentration at the ACL for completely passive operation at the anode uses product water from the cathode. For such a VDMFC system, pure MeOH can be used and energy densities for a complete system are increased.

The CCL and the membrane act as mass transport barriers and reduce water back diffusion. A partial ablation of the CCL can decrease this mass transport barrier. It was achieved by laser ablation of the catalyst layer, a process first proposed by Schmitz et al. [35]. The laser optics were focused on top of the CCL. Therefore, in particular the cathode side was ablated and the ACL remained mostly unsegmented. The actual pattern is shown in Fig. 13 with dimensions of $\Delta x = 571\ \mu m$ and $\Delta y = 577\ \mu m$ for each rectangle.

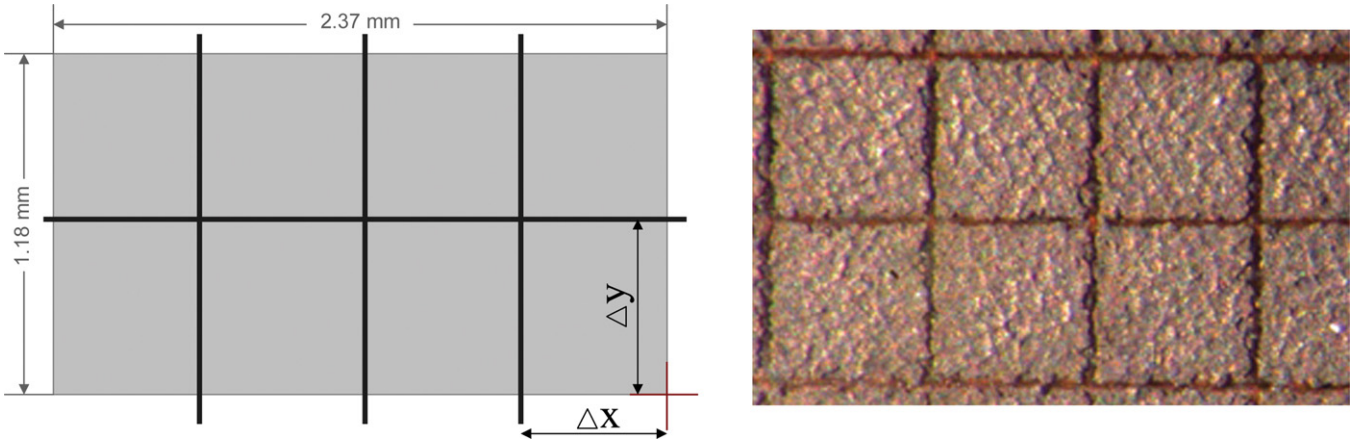

Fig. 13. Segmentation of the CCL to increase water back diffusion from cathode to anode. (a) Schematic drawing of the path of the laser beam. (b) Magnification of an ablated CCL.

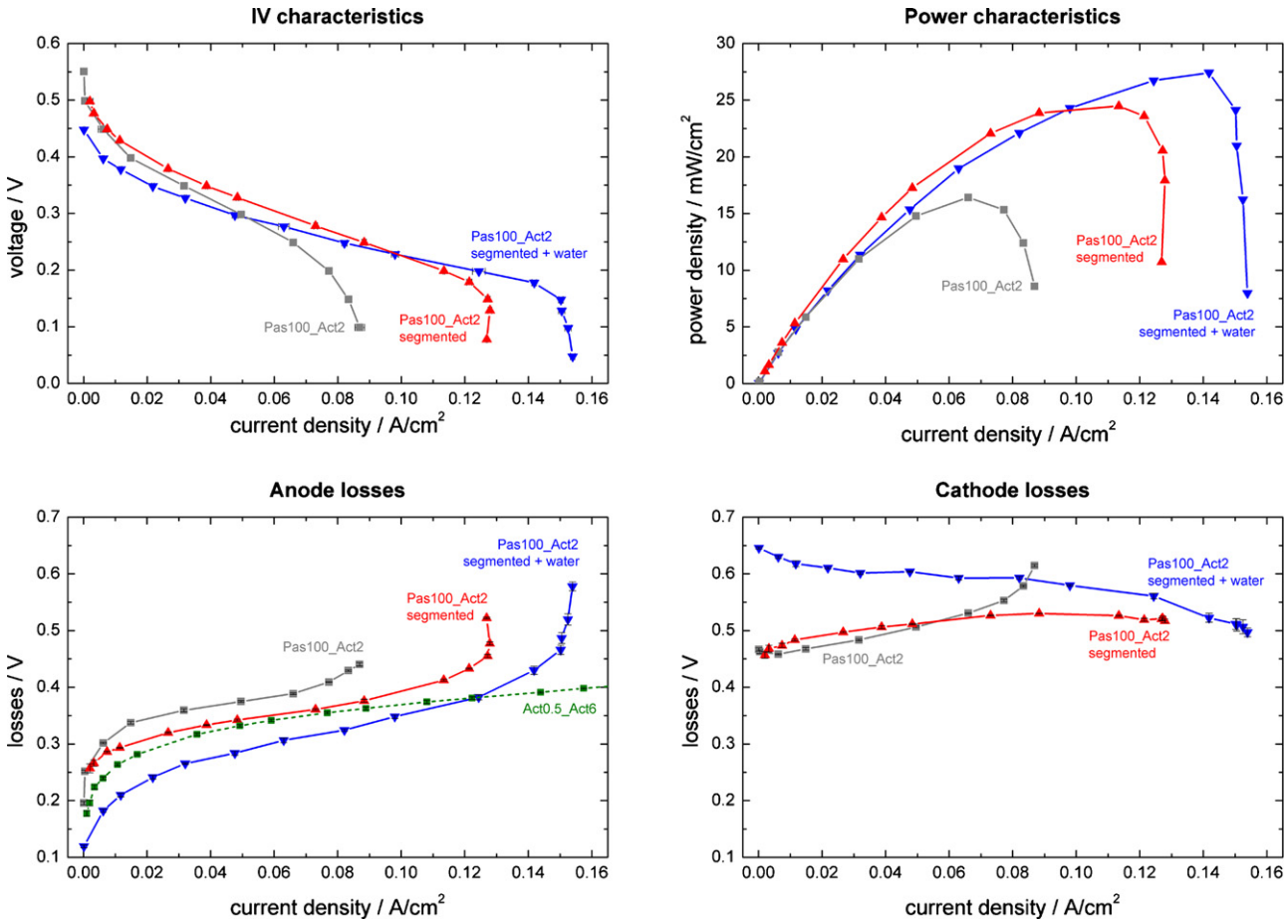

Fig. 14. Electric properties of a VDMFC for unsegmented and segmented CCLs and pure MeOH in the storage tank. Additional 0.5 ml of water was injected into the cathode air stream for "segmented + water". Anode and cathode polarization losses were calculated using a connected reference RHE. The temperature was 50 °C, the cathode air stream 40 sccm/ λ 2 and the evaporator opening ratio 6.8%. Additionally, anode losses for a LDMFC with properties according to Table 1 are shown.

The line width was limited by the laser optic and had a thickness of 30 μm. The active area of the CCL was reduced by 10% by the applied grid.

Experiments having an unsegmented cathode, a segmented cathode and a segmented cathode with externally applied water were performed. Pure MeOH within the storage tank was used with an opening ratio for the PDMS-membrane evaporator of 1.7% to keep crossover small. Air was supplied to the cathode at a stoichiometry of 2 with a minimum flow rate of 40 sccm. For these experiments a hydrophobic GDL with 20 wt% PTFE and including a microporous layer was assembled on the cathode side to keep water inside the electrode while 35 AA was used as the anode GDL.

The three cases according to the notation in Table 1 are compared in Fig. 14. Performance between the unsegmented and the segmented CCLs increased significantly and the limiting current density nearly doubled. It can be seen that anode losses of the unsegmented and the segmented CCL differ by 50 mV, a fact caused by higher water concentrations within the ACL. This conclusion was verified when additional 0.5 ml of water was injected into the segmented CCL and anode losses dropped further. On the other hand water injection into the cathode partially flooded the cathode and cathode losses increased. During the measurement water concentration at the CCL declined with time. Mass transfer of oxygen to the CCL improved and cathode losses decreased. At the same time water back diffusion to the anode diminished and anode losses raised.

Additionally, a comparison between vapor operation and a LDMFC with a 0.5 M solution of MeOH, a pump rate of 1 ml/min and a stoichiometry of 6 can be seen in Fig. 14. Anode polarization losses for the VDMFC with a segmented CCL were already comparable to the LDMFC up to a certain cell current density, where high concentration losses due to a lack of water occurred. With additional water added to the cathode, the VDMFC even outperformed the LDMFC with respect to anode polarization losses under the given operating conditions.

The ohmic high frequency resistance at 1 kHz and which is related to the water content of the membrane is depicted in Fig. 15. As expected from the electric properties, the resistance was lower for the segmented CCLs and decreased further when water was added to the cathode. A sharp increase of the ohmic resistance was recorded for the segmented CCL at 0.13 A cm^{-2}. Here less water could diffuse into the membrane than was consumed at the ACL and consequently the membrane was drying up. During the consecutive experiment when water was added to the segmented CCL it took some time for the membrane to get into a well humidified state again. Nevertheless, the ohmic resistance of 0.7 Ω cm^2 for the VDMFC was almost twice the resistance for the LDMFC at 0.4 Ω cm^2, which supports the conclusion that the water uptake of the membrane is higher when in contact with a liquid [36–38].

It can be concluded that water management is the critical issue for a VDMFC. Excess water at the cathode limits the oxygen mass transport to the CCL. Low cathodic water concentrations reduce water back diffusion to the ACL, a fact that reduces performance significantly when operating the VDMFC at high MeOH concentrations.

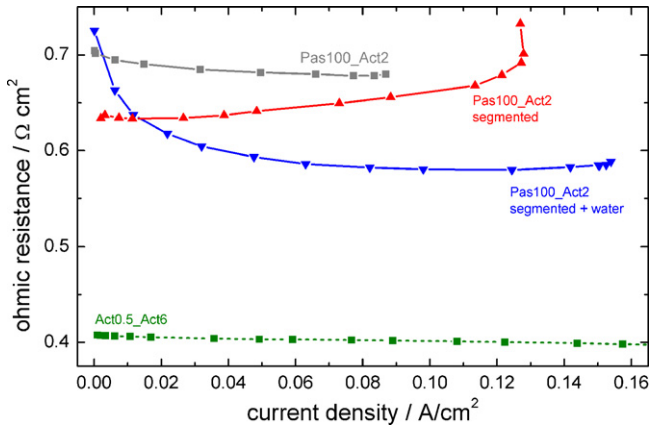

Fig. 15. Ohmic resistance of the VDMFC versus current density for unsegmented and segmented CCLs. Additional 0.5 ml of water was injected into the cathode air stream for "segmented + water". The temperature was 50 °C, the cathode air stream 40 sccm/ λ 2 and the evaporator opening ratio 6.8%. Additionally, ohmic resistances for a LDMFC with properties according to Table 1 are shown.

3.4. Efficiency

The efficiency of a fuel cell system is a convenient parameter to make comparison to other electrochemical systems, e.g. primary or secondary batteries. In this section heat production of a VDMFC is looked at. Additionally, Faradaic and voltage efficiencies are evaluated for different structural parameters and operating conditions.

3.4.1. Heat losses

During the electrochemical reactions, MOR at the anode and ORR at the cathode, heat is generated. The common convention that heat production has a negative sign and heat consumption a positive sign, is used. The enthalpy change of the DMFC is calculated with values of [39]($\Delta H_{DMFC} = -726.51$ kJ/mol). The cell voltage U is taken from the respective working point:

$$-q_{DMFC} = -i\left(\frac{\Delta H_{DMFC}}{6F} + U\right) \quad (4)$$

An additional term has to be added that accounts for MeOH crossover which is parasitically oxidized at the cathode. It equals Faradaic losses in the case of a VDMFC with a closed fuel cartridge. For simplicity it is assumed that all MeOH at the cathode is electrochemically oxidized with a six-electron transfer process:

$$-q_{CO_2} = -i_{leak}\frac{\Delta H_{DMFC}}{6F} \quad (5)$$

The leakage current density i_{leak} describes the equivalent current density of MeOH crossover. Using Eqs. (4) and (5) the total heat output can be calculated:

$$-q_{tot} = -q_{DMFC} - q_{CO_2} = -i\left(\frac{\Delta H_{DMFC}}{6F} + U\right) - i_{leak}\frac{\Delta H_{DMFC}}{6F} \quad (6)$$

Among other effects, MeOH crossover is highly dependent on the fuel cell temperature. Fig. 16 shows power densities and heat losses of the fuel cell and MeOH crossover for three different temperatures. A screen-printed CCM having Nafion® 117 as a membrane with 3 mg cm^{-2} Pt/Ru at the anode and 1 mg cm^{-2} Pt at the cathode

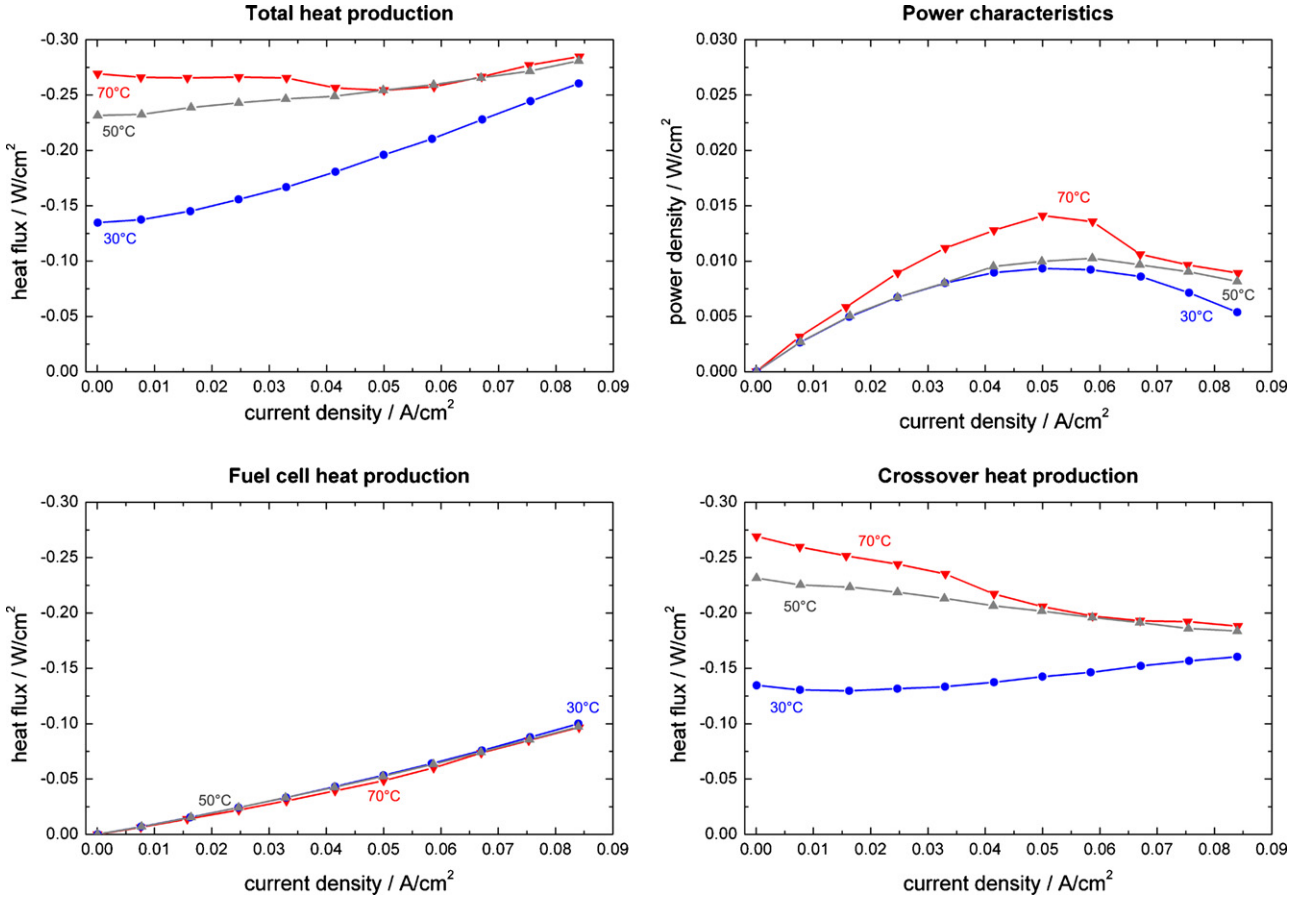

Fig. 16. Heat fluxes and power densities of a VDMFC for different temperatures. The cathode air stream was 30 sccm/ λ 2 and the evaporator opening ratio 1.7% with a 75 wt% solution of MeOH.

attached to non-teflonized GDLs was used. Cathode stoichiometry was 2 with a minimum air stream of 30 sccm. A 75 wt% solution of MeOH was evaporated through a PDMS membrane with an opening ratio of 1.7%.

It can be noted in the graph that the highest difference in heat production between the temperatures was gained at OCV, when heat production of the fuel cell is least. Crossover of MeOH across the membrane causes a heat production that is significantly higher than the heat of the fuel cell losses. Therefore, even for 30 °C, a heat output of 140 mW/cm^2 remained at OCV. This means that a large amount of fuel is consumed while the fuel cell is on "Standby". Consequently, a mechanical separation between the storage and the anode vapor chamber has to be considered for VDMFC systems.

On the other hand, heat production can be of advantage for non-isothermal operation of a VDMFC system. As can be seen in the graph heat production at 70 ° C remained relatively constant at different current densities. While fuel cell losses increased with current density MeOH crossover declined so that the superposition of these two heat sources according to Eq. (6) stabilized. It was shown in the parameter study Section 3.1 that temperatures between 50 and 70 ° C increase the performance drastically compared to ambient conditions. Heat production can be used to keep a VDMFC system at elevated temperatures. This would also decrease the risk of freezing at temperatures below freezing point for outdoor applications.

3.4.2. Total efficiency

Extended-duration experiments at a constant current were performed to gain knowledge about system efficiencies of the VDMFC test cell. Most conditions of the Parameter study section were applied: PDMS-membrane, 50 ° C and a non-teflonized GDL. Nafion® 117 with an Pt/Ru anode loading of 3 mg cm^{-2} and a Pt cathode loading of 1 mg cm^{-2} was used. The thermodynamic efficiency is defined as

$$\eta_{\text{th}} = \frac{\Delta G}{\Delta H} \tag{7}$$

whereas the voltage efficiency is defined as

$$\eta_u = -\frac{6FU}{\Delta G} \tag{8}$$

The total efficiency η_{tot} can be derived experimentally:

$$\eta_{\text{tot}} = \eta_i \eta_u \eta_{\text{th}} = \frac{I\bar{U}\Delta t}{n_{0,\text{MeOH}}\Delta H_{\text{MeOH}}} \tag{9}$$

and in consequence the Faradaic efficiency η_i can be calculated.

A 50 wt% solution of MeOH in deionized water was used for this experiment with forced air flow at a stoichiometry of 2. The opening ratio of the evaporator was 6.8%. The external load drew a constant current of 90 mA cm^{-2}, which was close to the MPP, from the fuel cell. After a time $\Delta t \approx 2.8$ h voltage dropped to zero and no power could be drawn from the cell. Averaging current and voltage in this period the Faradaic, voltage and total efficiencies could be obtained.

Faradaic, voltage and total efficiencies for the four experiments can be seen in Fig. 17. Fuel crossover, fuel losses through the outlet vent for $CO_2$and residual concentrations caused a Faradaic efficiency of only 60% and below.

The OCV of a DMFC is strongly reduced compared to its theoretical value, mostly because of the mixed potential at the cathode electrode. At the working point, if MeOH is not totally consumed inside the ACL during the MOR, crossover occurs and the same mechanism that reduces OCV leads to smaller cell potentials. Therefore, the voltage efficiency is usually quite low for DMFCs. This conclusion is also valid for the given conditions of the VDMFC, and the voltage efficiencies are slightly above 10%.

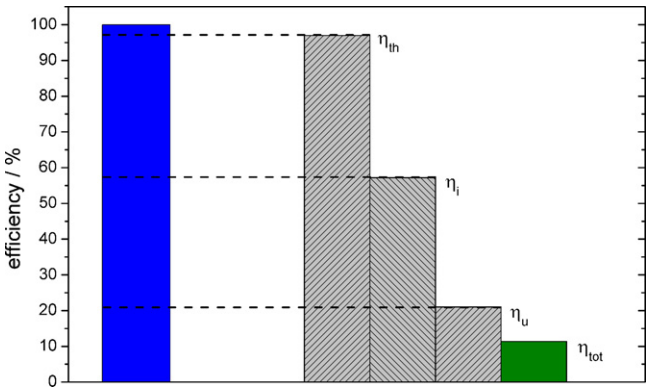

Fig. 17. Thermodynamic, Faraday, voltage and total efficiency of a VDMFC (50 wt%) with a forced cathodic air flow of 40 sccm. Efficencies are calculated according to Eqs. (6)–(8). Temperature was set to 50 °C, the opening ratio was 6.8%.

In conclusion, MeOH crossover strongly affects both, Faradaic and voltage efficiency. Working points where most of the MeOH is consumed at the anode electrode in addition to membrane materials that reduce crossover flux of MeOH are needed to increase system efficiencies.

4. Conclusions

A novel concept having a passively fed anode, which in combination with air-breathing cathodes would allow for complete passive operation of a DMFC, was introduced. A phase separation membrane separated liquid methanol in the storage tank from the gaseous methanol in the anode chamber. Methanol supply to the anode was driven by adsorption, transport and desorption of methanol through the membrane. Several structural parameters, like the choice of GDL materials, and operating conditions, like temperature or air stoichiometry at the cathode, were looked at.

Water concentration at the anode electrode was found to be a major factor that influenced performance of the vapor-fed direct methanol fuel cell significantly. Water transport to the anode electrode was mainly caused by a large concentration gradient between the anode and the cathode. Therefore, all actions that reduced water concentration at the cathode, such as increased air flow rates at the cathode or decreased methanol concentrations at the anode resulting in lower methanol crossover, limited the performance and especially the limiting current density of the fuel cell.

The effective evaporation area was identified to be an important factor that interacts with the methanol concentration in the liquid reservoir, fuel cell performance and crossover of methanol across the membrane. It was shown that operation with pure methanol was possible, as product water from the cathode diffused back through the ionomer to the anode as a reactant. As already mentioned, water supply to the anode electrode is a critical issue for vapor-fed DMFCs. Back diffusion of cathodic product water was enhanced by introducing hydrophobic layers at the cathode side and by partial ablation of the cathode catalyst layer. Faradaic and voltage efficiencies including heat production by the parasitic methanol oxidation at the cathode were determined. The heat flux of a vapor-fed DMFC was one order of magnitude higher than the produced electric power density. The total efficiency was found to be approximately 12%.

References

[1] C. Dyer, Journal of Power Sources 106 (2002) 31–34.

[2] A. Heinzel, C. Hebling, M. Muller, M. Zedda, C. Muller, Journal of Power Sources 105 (2) (2002) 250–255.
[3] P. Gravesen, J. Branebjerg, O. Soendergaard Jensen, Journal of Micromechanics and Microengineering 3 (4) (1993) 168–182.
[4] D.J. Laser, J.G. Santiago, Journal of Micromechanics and Microengineering (6) (2004) R35.
[5] A. Shukla, P. Christensen, A. Hamnett, M. Hogarth, Journal of Power Sources 55 (1) (1995) 87–91.
[6] A. Arico, P. Creti, R. Mantegna, P. Antonucci, N. Giordano, V. Antonucci, Journal of the Electrochemical Society 143 (12) (1996) 3950–3959.
[7] M. Hogarth, P. Christensen, A. Hamnett, A. Shukla, Journal of Power Sources 69 (1–2) (1997) 125–136.
[8] H. Fukunaga, T. Ishida, N. Teranishi, C. Arai, K. Yamada, Electrochimica Acta 49 (2004) 2123–2129.
[9] K. Furukawa, F. Kaga, K. Okajima, M. Sudoh, International Journal of Green Energy 1 (1) (2004) 123–135.
[10] J. Kallo, W. Lehnert, R. von Helmolt, Journal of the Electrochemical Society 150 (6) (2003) A765–A769.
[11] J. Kallo, J. Kamara, W. Lehnert, R. Helmolt, Journal of Power Sources 127 (2004) 181–186.
[12] M. Abdelkareem, N. Nakagawa, Journal of Power Sources 162 (1) (2006) 114–123.
[13] L. Fuqiang, L. Guoqiang, W. Chao Yang, Journal of the Electrochemical Society 153 (3) (2006) A543–A553.
[14] N. Nakagawa, M.A. Abdelkareem, K. Sekimoto, Journal of Power Sources 160 (1) (2006) 105–115.
[15] W.-J. Kim, H.-G. Choi, Y.-K. Lee, J.-D. Nam, S.M. Cho, C.-H. Chung, Journal of Power Sources 157 (1) (2006) 193–195.
[16] X. Feng, R.Y.M. Huang, Industrial & Engineering Chemistry Research 36 (4) (1997) 1048–1066.
[17] H. Kim, Journal of Power Sources 162 (2) (2006) 1232–1235.
[18] J. Guo, W.-C. Huang, B.Z. Jang, A new highly-efficient direct methanol fuel cell, in: Proceedings of the International Conference on Fuel Cell Science, Engineering, and Technology, 4th, Irvine, CA, United States, June 19–21, 2006 Pt. B, 2006, pp. 1099–1103.
[19] Z. Guo, A. Faghri, Journal of Power Sources 167 (2) (2007) 378–390.
[20] S. Eccarius, T. Manurung, C. Ziegler, Journal of the Electrochemical Society 154 (8) (2007) B852–B864.
[21] F. Meier, S. Denz, A. Weller, G. Eigenberger, Fuel Cells 3 (4) (2003) 161–168.
[22] W. Vielstich, V.A. Paganin, F.H.B. Lima, E.A. Ticianelli, Journal of the Electrochemical Society 148 (5) (2001) A502–A505.
[23] H. Dohle, J. Divisek, J. Mergel, H. Oetjen, C. Zingler, D. Stolten, Journal of Power Sources 105 (2) (2002) 274–282.
[24] Z. Qi, A. Kaufman, Journal of Power Sources 110 (1) (2002) 177–185.
[25] A.Z. Weber, J. Newman, Journal of the Electrochemical Society 151 (2) (2004) A311–A325.
[26] J. Cowart, Journal of Power Sources 143 (2005) 30–35.
[27] N. Nakagawa, Y. Xiu, Journal of Power Sources 118 (2003) 248–255.
[28] K. Scott, W.M. Taama, P. Argyropoulos, Journal of Applied Electrochemistry 28 (12) (1998) 1389–1397.
[29] J. Amphlett, B. Peppley, E. Halliop, A. Sadiq, Journal of Power Sources 96 (1) (2001) 204–213.
[30] C. Chen, P. Yang, Journal of Power Sources 123 (2003) 37–42.
[31] T. Yen, N. Fang, X. Zhang, G. Lu, C. Wang, Applied Physics Letters 83 (9) (2003) 4056–4058.
[32] S. Eccarius, B. Garcia, C. Hebling, J. Weidner, Experimental validation of a methanol crossover model in DMFC applications, Journal of Power Sources 179 (2) (2008) 723–733.
[34] X. Ren, W. Henderson, S. Gottesfeld, Journal of the Electrochemical Society 144 (9) (1997) L267–L270.
[35] A. Schmitz, S. Wagner, R. Hahn, A. Weil, E. Schneiderloechner, M. Tranitz, C. Hebling, Fuel Cells 4 (3) (2004) 1–6.
[36] P. von Schroeder, Physikalische Chemie 45 (1903) 75–117.
[37] A.Z. Weber, J. Newman, Journal of the Electrochemical Society 150 (7) (2003) A1008–A1015.
[38] C.M. Gates, J. Newman, AIChE Journal 46 (10) (2000) 2076–2085.
[39] P. Atkins, Physical Chemistry, 3rd ed., Oxford University Press, 1986.